

INSTITUT POLYTECHNIQUE DES SCIENCES AVANCÉES<sup>1</sup>  
Paris, France

ROYAL OBSERVATORY OF BELGIUM<sup>2</sup>  
Brussels, Belgium



---

**MASTER PROJECT REPORT**  
**Simulation of thermal camera images from a spacecraft around asteroid for**  
**the HERA mission**

---

*Author*

**Jordan Culeux<sup>1</sup>**  
**Grégoire Henry<sup>1</sup>**  
**Théo Mercurio<sup>1</sup>**  
**Georges-Antoni Moubayed<sup>1</sup>**

*Supervisor*

**Özgür Karatekin<sup>2</sup>**  
**Elodie Glosesener<sup>2</sup>**



## Abstract

Didymoon is an asteroid of the binary system Didymos. It is orbiting around a bigger asteroid called Didymain for convenience. In order to prepare the defense of the Earth in the case of a direct impact of an asteroid, the Hera mission will initiate in the years to follow an impact onto Didymoon. The NASA is in charge of the collision with the asteroid. The ESA will study the outcomes of the impact. The spacecraft Hera will be equipped of sensors such as cameras. Studying the evolution of the temperature on Didymoon will help us to understand what happened to after the collision. This work fits into the scheme of the simulations of thermal camera images from the spacecraft around the asteroid. This paper shows a method using asteroid thermophysical model, 3D numerical solver, NASA/NAIF SPICE and shape models.

## 1. The Hera mission

Cruising some 250 million kilometers around the Sun is an object first identified in 1996 as 1196G, by a Spacewatch survey at the University of Arizona. It was later named Didymos (Greek word for twin), after a smaller companion, Didymoon, was discovered orbiting it. Didymos is now classified as a potentially hazardous, near-Earth system. Hera, named after the greek goddess of marriage, will be humanity's first probe to rendezvous with a binary asteroid system.

Hera is part of an international collaboration, alongside Nasa's DART which is due to deliver a kinetic impact Didymoon's surface, leading to a deflection of its orbit around the bigger brother.

The mission's main objectives are to deepen our understanding of a planetary defense technique while also demonstrating numerous technologies, the likes of autonomous navigation around asteroids and gathering scientific data, further developing our understanding of asteroid compositions and structures.

Hera is set to launch in 2024, before traveling to Didymos where it will first focus on Didymoon for its study: High resolution mapping relying on Optical, radio and laser techniques.

In addition to planetary defense objectives, Hera will also carry two CubeSats on board, to be launched around the asteroid system for crucial scientific studies before touching down on their surface.

In this paper, we describe our contribution to

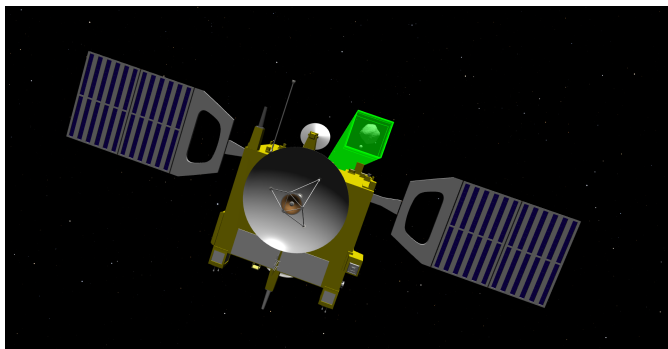


**Figure 1:** The binary system of asteroids Didymos viewed from the spacecraft Hera. The field of view of the AFC camera is in green.

the Hera Mission. Our work on the thermophysical model consists of taking into consideration the self heating (heat flux reflected from Didymoon's own 3D relief) and mutual heating (heat flux from Didymain) phenomena. Geometric considerations were further made to enrich the model such as true position, obliquity (with NASA/NAIF Spice) and shape models.

## 2. Current work

This paper is following the work of a previous document *Didymoon's surface thermal modeling*. The former presents a method to simulate the temperature at the surface of an asteroid. It describes in details the following thermophysical model and the numerical method:

$$\begin{cases} u(x, 0) = f(x), & \forall x \in [0, l_s] \\ \frac{\partial u}{\partial x}(0, t) = \frac{Q_{out} - Q_{\odot}}{k} & \forall t \geq 0 \\ \frac{\partial u}{\partial x}(l_s, t) = 0, & \forall t \geq 0 \end{cases} \quad (1)$$

with  $u$  the 1 dimensional temperature in space and time,  $f$  initial temperature repartition,  $Q_{out}$  the flux emitted from the asteroid,  $Q_{\odot}$  the flux received from the Sun,  $k$  the conductivity and  $l_s$  the annual thermal skin depth. The expression of  $Q_{out}$  is:

$$Q_{out} = \epsilon \sigma u^4 \quad (2)$$

with  $\epsilon$  the emissivity of the asteroid and  $\sigma$  the Stephan-Boltzman constant.  $Q_{\odot}$  is stated as:

$$Q_{\odot} = \frac{S_{\odot} (1 - A) \cos \varsigma}{r^2} \quad (3)$$

with  $S_{\odot}$  the solar constant heat flux,  $A$  the bond albedo of the asteroid,  $\varsigma$  the incidence angle and  $r$  the heliocentric distance in AU. The annual thermal skin depth is written as:

$$l_s = \sqrt{\alpha \pi p} \quad (4)$$

where  $\alpha$  is the diffusivity and  $p$  is the orbital period. The diffusivity is expressed as:

$$\alpha = \frac{k}{\rho c} \quad (5)$$

where  $\rho$  is the density and  $c$  the heat capacity. The second equation of this thermophysical model is the heat flux at the surface of the asteroid and the third is an adiabatic condition set at several annual thermal skin depth. This model is based on the heat transfer equation:

$$\frac{\partial u}{\partial t} = \alpha \frac{\partial^2 u}{\partial x^2} \quad (6)$$

This ensures the conduction of the temperature inside the asteroid. To express the temperature from this equation, we used a second order finite-difference method and iterative techniques such as the Newton method. During the process, we defined the numerical stability parameter:

$$S = \alpha \frac{\Delta t}{\Delta x^2} \quad (7)$$

This parameter must remain lower than 0.25 for stability purposes. For the simulations, it is important to define the thermal inertia:

$$\Gamma = \sqrt{k\rho c} \quad (8)$$

### 3. Objectives

Following the former document, the main objective of this paper is to have a more complex thermophysical model to get closer to the reality. The heat flux from the Sun is the main source of heating for asteroids but there are more phenomena happening to implement

and especially for a binary system of asteroids. Of all second day heating modes, mutual heating is the most important. Another effect to implement for craters or rough-shape asteroids is the self heating. This paper also aims to present a method to include the asteroid obliquity in our model. The document is mainly focused on the study of Didymos's secondary object Didymoon but it also presents another planetary defense mission with very different orbital and asteroid parameters and is interesting for comprehension purposes.

### 4. A thermophysical model for a binary system of asteroids

In this section, we present the implementation of the mutual heating. As Didymos is a binary system of asteroids, the current thermophysical model is not enough to fully describe the temperature at the surface of the asteroid. The Hera mission focuses on the secondary object in this binary system. Its surface temperature also depends on the primary object for two main reasons. Firstly, the reflection of the Sun on the surface of the primary to the secondary, this phenomenon relies on the primary body's albedo and on its position with respect to the Sun and to the secondary, and this is referred to mutual direct heating. Secondly, the heat received from the primary itself, just as the Sun, considering it as a black body, it only depends on the distance and is referred to mutual diffuse heating.



**Figure 2:** The binary system of asteroid Didymos



**Figure 3:** (1) View factor on Didymos system and (2) View factor schematic interpretation

#### 4.1. Theory

Didymos' secondary is modeled in a simplified manner due to the many unknowns and assumptions adopted in this study. This section deals with neglected effects thought to alter surface temperatures in certain cases.

A complete thermophysical model including the direct and diffuse mutual heating is (Pelivan et al., 2017):

$$Q_{\odot} + W_p + Q_p + W_m + Q_m = \epsilon\sigma u^4 - k \frac{\partial u}{\partial x} \Big|_{x=0} \quad (9)$$

where  $W_p$  stands for the mutual heating from diffuse solar radiation from the primary,  $Q_p$  corresponds to the direct thermal heating from the primary considered as a black body,  $W_m$  is the diffuse thermal self heating,  $Q_m$  is the direct thermal self heating and  $\partial u/\partial x$  is the vertical temperature gradient with  $x$  positive upward.

For the current simplified model, the mutual heating from Didymain to Didymoon will be small due to the comparatively large distance of 1.18 km (Didymos reference model) between the two bodies. As defined in the reference model, the low albedo allows us to apply the single-scattering mode for which the diffuse thermal self heating flux  $W_m$  can be neglected. Furthermore, considering the current shape of Didymoon, which is a simple ellipsoid, it is not necessary to include the term  $Q_m$  neither. However, these two flux will be discussed in the next part.

Discretizing the two bodies into facets  $i$  for the secondary and  $j$  for the primary, the mutual heating from diffuse solar radiation from the primary can be computed using:

$$W_p = \sum_{i \neq j}^N V_{ij} \frac{S_{\odot} A \cos \zeta_j}{r_H^2} \quad (10)$$

Where  $N$  is the total number of facets and  $V_{ij}$  is the view factor expressed as:

$$V_{ij} = \frac{a_i \cos \theta_i \cos \theta_j}{\pi r^2} \quad (11)$$

where  $a_i$  is the surface area of the seconday,  $r$  is the distance between facets  $i$  and  $j$  and angles  $\theta$  are the angles between the facet outward normal and the line

between facet centers from primary and seconday. An angle of  $\theta \geq 90$  degrees represents two facets not facing each other. Schemes in Fig. 3 explain the situation.

Due to low albedo (both albedos of the primary and secondary are assumed identical) the direct thermal heating  $Q_p$  is the largest flux from the primary:

$$Q_p = \sum_{i \neq j}^N V_{ij} \epsilon \sigma u_j^4 \quad (12)$$

where  $u_j$  is the surface temperature of facet  $j$ . For computing time purposes, temperatures of the primary are not computed. All facets temperatures  $u_j$  are set to the highest midday temperature of the moon.

#### 4.2. Integration

The Eq. 9 can now be implemented to the current thermophysical model in Eq. 1 to include the mutual heating from the primary body of the binary system of asteroids Didymos. Surface temperatures have been computed to each single node from the ESA shape models of the Didymos system asteroids.

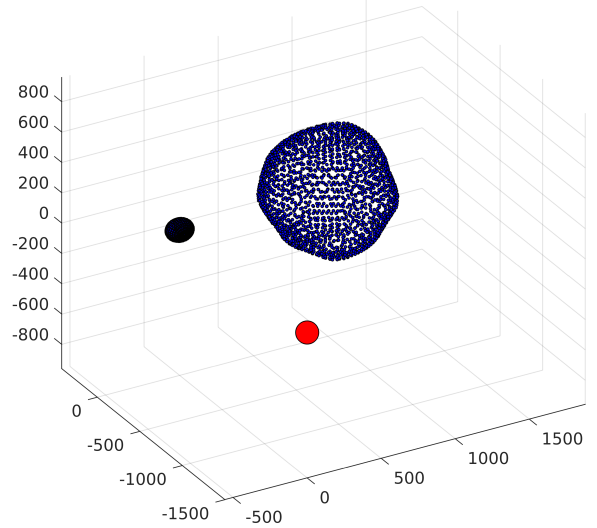


**Figure 4:** The binary system of asteroids Didymos with the Sun direction. Latest shape models of the ESA have been used in this simulation. The primary has a radius of 500 meters and the secondary 80 meters.

After implementation of Didymoon's revolution, the following results are obtained for the surface temperatures of the secondary including the mutual heating from the primary:

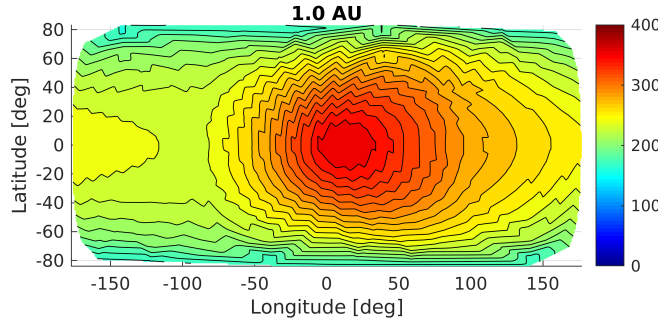


**Figure 5:** Thermal map of the secondary of the binary system of asteroids Didymos including the mutual heating from the primary using ESA shape models.

The computations were realized without the implementation of the obliquity, which is discussed in further sections. To compare with the previous implementation in Eq. 1, this graphs shows the benefits of including the mutual heating:

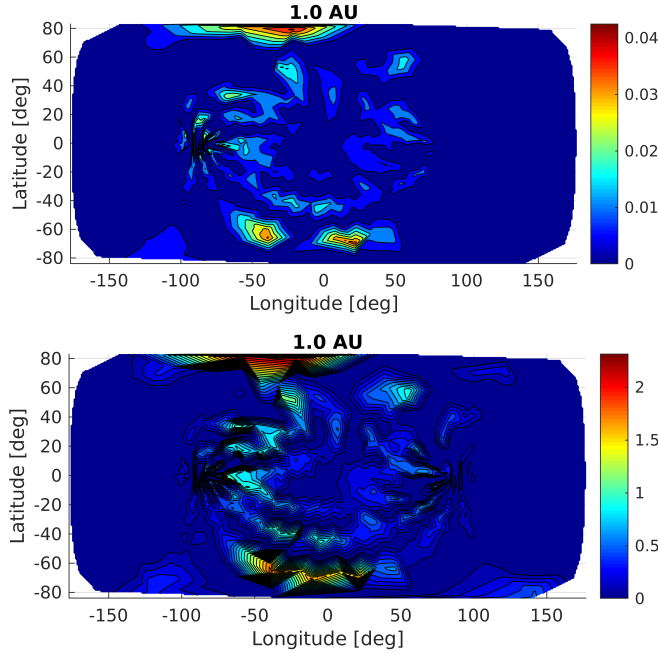


**Figure 6:** The two graphs show the impact of including the mutual heating on the surface temperatures of Didymoon. The first figure shows the difference between the surface temperatures with the secondary diffuse mutual heating only (Eq. 10) and without it. The second image is the difference of temperature including the two equation of the mutual heating (Eq. 10 & Eq. 12) and without it.

The assumptions which consisted of considering the direct mutual heating as the largest flux of the mutual is confirmed with this graph. Furthermore, the Eq. 10 costs much more computational time than the Eq. 12, thus, and due to the present albedo, it might be more clever to not implement it. The first case suggests an increase of 0.05 K where the second case represents an increase of more than 2 K depending on the region.

### 4.3. Parameters

Orbital parameters and asteroid properties are considered identical to the [Didymos reference model](#) and [Michel et al. \(2016\)](#).

Table 1  
Asteroid parameters

Parameter	Value
Orbital period	11.92 h
Revolution period	11.92 h
Thermal inertia	$500 \text{ J K}^{-1} \text{ m}^{-2} \text{ s}^{1/2}$
Density	$2146 \text{ kg m}^{-3}$
Heat capacity	$600 \text{ J K}^{-1}$
Bond albedo	0.07
Emissivity	0.9
Obliquity	$171 \pm 9^\circ$

## 5. Advanced thermophysical model for rough surface including craters

This section shows the implementation of the self heating. A normal at the surface of an asteroid may appear to be hidden from the direct solar flux even if it is situated in the day side, for instance inside a crater. In this scenario, it is important to take into consideration what is called the self heating of the asteroid. Due to its albedo, the surface of the asteroid reflects sunlight rays and thus, if the asteroid is not purely smooth, some reflected rays might impact another location on the asteroid resulting in heating it up.

### 5.1. Theory

The implementation of the thermophysical model beaming into Didymoon, described in [section 4](#), had mutual-heating occurring between the two bodies of the Didymos system. However, this implementation neglected global self heating that can occur within large-scale concavities of an irregularly shaped asteroid.

Global self-heating provides a mechanism for heat to be transferred laterally across an asteroid surface. [Fig. 7](#) demonstrates how global self heating can affect the thermophysical model and temperatures predictions for an asteroid with a large-scale concavity and an irregular shape. The large-scale concavity results in heat transfers that occur at certain geometries, where a facet is facing another one. In the absence of global self heating, those facets would receive only direct flux and mutual heating flux. However, if the facet receives reflected solar flux and emitted thermal radiation from the opposite side of the concavity that is illuminated, the temperature would be higher than expected. The aim of this section is to implement this phenomenon.

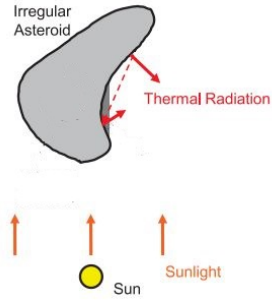


**Figure 8:** Schematic of global self-heating occurring inside a large concavity of an asteroid.

In the specific case of Didymoon, its shape model is still incredibly simple. The ESA's shape for Didymoon is a smooth ellipsoid. This leads in the total absence of self heating. For this purpose, a more complex shape model has been taken, Mathilde, visible in Fig. 9.

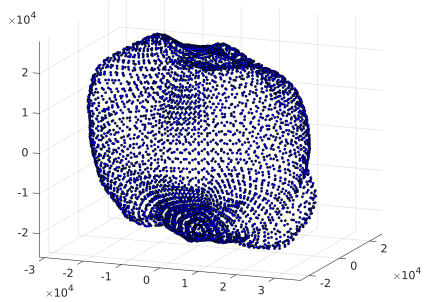


**Figure 9:** Shape model of the asteroid Mathilde. Dimensions: 66x48x46 km.

The two terms relative to the self heating in Eq. 9 are now considered following:

$$W_m = \sum_{i_1 \neq i_2}^N V_{i_1 i_2} \frac{S_\odot A \cos \varsigma_{i_2}}{r_H^2} \quad (13)$$

$$Q_m = \sum_{i_1 \neq i_2}^N V_{i_1 i_2} \epsilon \sigma u_{i_2}^4 \quad (14)$$

These two equations complete the model seen in Eq. 9. They are very similar to the mutual heating. The only

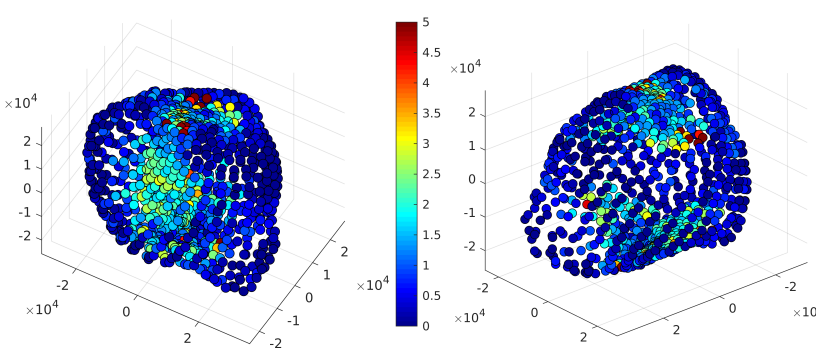
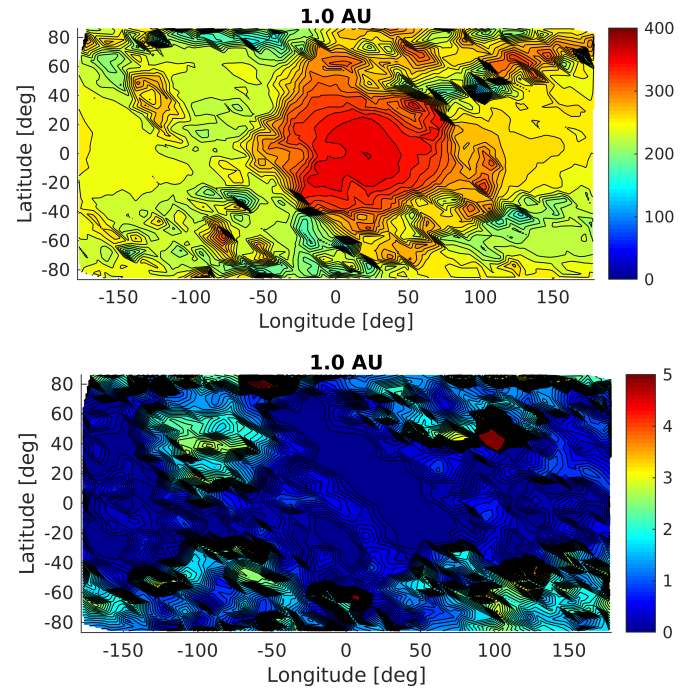


**Figure 7:** Self heating contribution displayed on the 3D shape model of the asteroid Mathilde.

difference is the indices of the facets. Each surface node temperature is computed with respect to every other node on the asteroid except the current one.  $i_1$  and  $i_2$  belong to the asteroid.  $V_{i_1 i_2}$  is computed as seen in Eq. 11. Same assumptions are made for  $u_{i_2}$  as in the section 4.

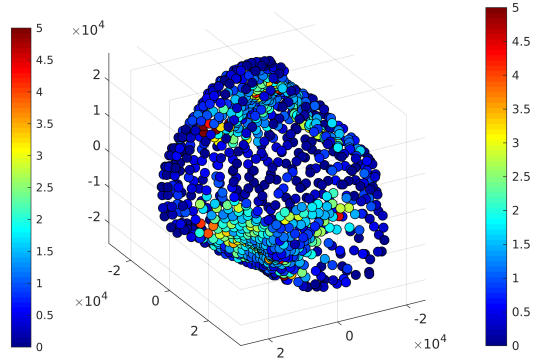
## 5.2. Integration

To investigate in general how global self heating within large concavities of asteroids influences thermophysical model, it is needed to first check the result's consistency, such as the surface temperature expected to be higher in a crater. The implementation of the self heating on the shape model of the asteroid Mathilde results in the thermal map in Fig. 10.



**Figure 10:** The first figure is the thermal map of the surface of the asteroid Mathilde including its self heating. The second figure is the contribution of the self heating on thermal map. Orbital parameters and asteroid properties are taken as in section 4.

The contribution of the self heating may appear to be



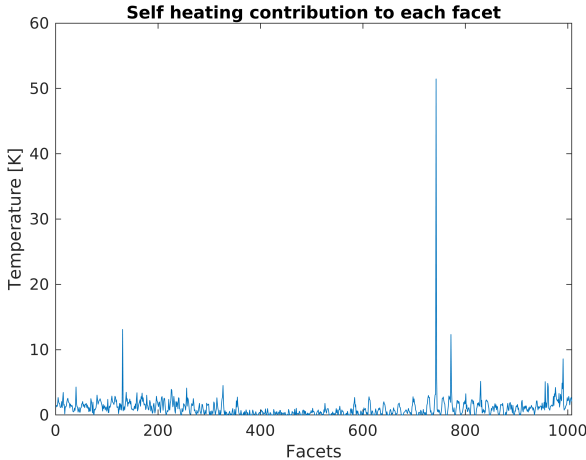


**Figure 11:** Distribution of the self heating contribution for each facet. Most values are located between 0 and 5 Kelvin.

in some places higher than 5 Kelvins, as shown in Fig. 11, but this color axis has been chosen for reading purposes.

Results in Fig. 7 appear to be consistent. The self heating distribution of the contribution is mostly located in craters. The roughness of the asteroid also contributes in the creation of self heating.

## 6. Another important celestial parameter: the obliquity

This section describes the implementation of the obliquity and an explanation of its impact on surface temperatures. Obliquity is defined as the angle of tilt of the body's axis of rotation. Thus, it has an immediate impact on the repartition of temperatures on the body as this figure describes:

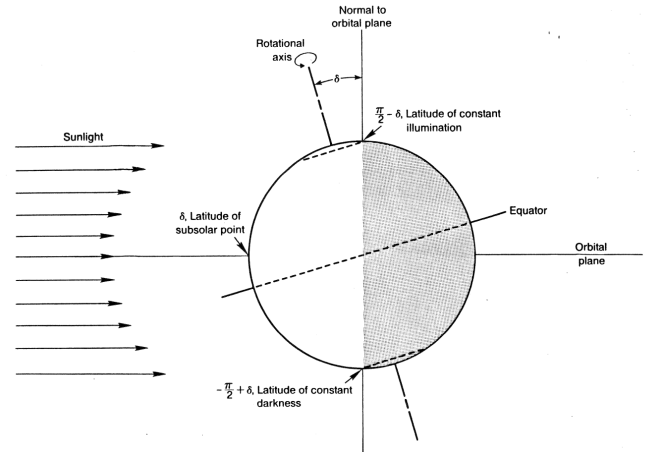


**Figure 13:** Representation of the obliquity with the orbital plane and the rotational axis

From the obliquity results two observable events. First, the subsolar point is not anymore located on the equator but on a point tilted from the equator as the figure shows above. Secondly, depending on the position of the asteroid on its orbit - i.e. depending on the seasons, only one pole is not receiving direct heating from the Sun whereas without obliquity both poles are not receiving the heat.

Before running the simulations presented in the previous sections, we implement the axial tilt on the shape model.

Demonstration of the effects of the obliquity are performed for the temperature evolution of Didymos' secondary along a full day assuming an ellipsoidal shape.

As expected, temperature peaks shift in latitudes depending on the obliquity and the south pole only is in the cold zone.

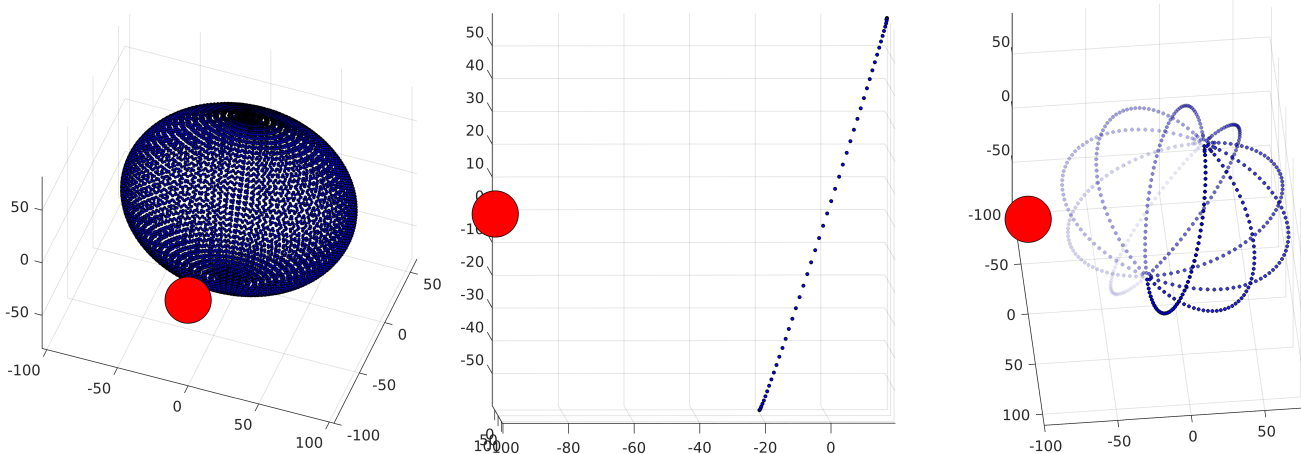


**Figure 12:** Implementation of the obliquity for the daily surface temperature variation at longitude = 0 degrees on Didymos' secondary. The spin axis is given as  $171 \pm 9$  degrees. Here, the extreme case of 162 degrees has been considered. The first figure is Didymo's shape with obliquity and the direction of the Sun. On the second image we show only the meridian at longitude 0. The third pictures the rotation of the meridian during a day.

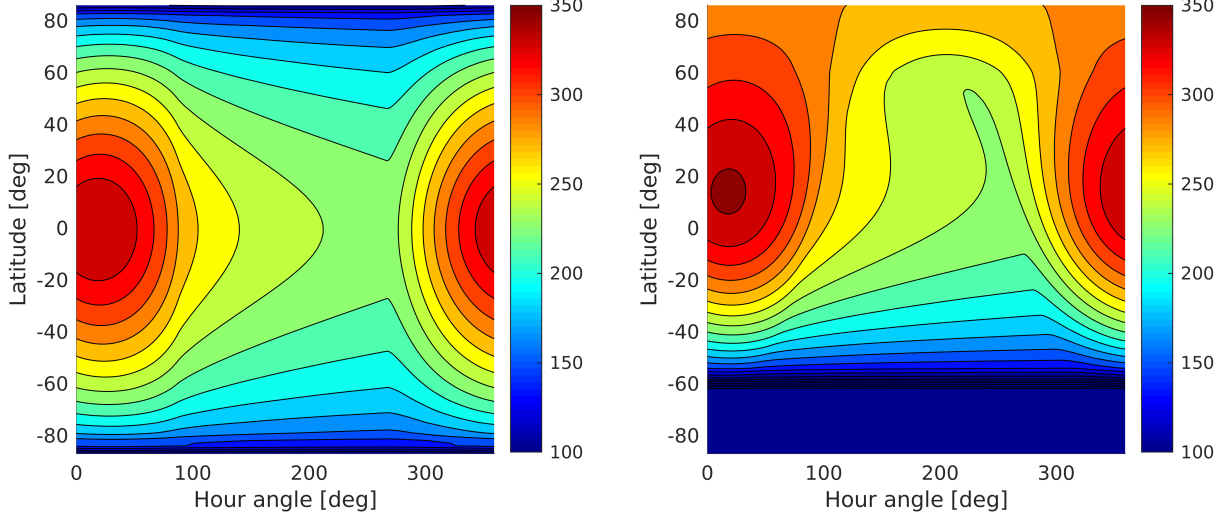


**Figure 14:** Contour maps of the daily surface temperature variation at longitude = 0 degree on Didymos' secondary for a thermal inertia of  $\Gamma = 500 \text{ Jm}^{-2}\text{K}^{-1}\text{s}^{-1/2}$ , an heliocentric distance of 1.0748 AU and 162 degrees of obliquity.

## 7. Another planetary defense mission: 2016 HO3

This section introduces another scientific mission, which interests people for its particularity. (469219) Kamo'oalewa, provisionally designated 2016 HO3, is a quasi-satellite of the Earth, i.e. the asteroid stays always close to the Earth but it is orbiting around the Sun. It was discovered on April 27, 2016 by the Pan-STARRS program at the Haleakala observatory on the Hawaiian island of Maui. Its main specificity is its fast revolution period of 20 minutes. Studying this asteroid is relevant to understand the impact of its revolution period on its temperature.

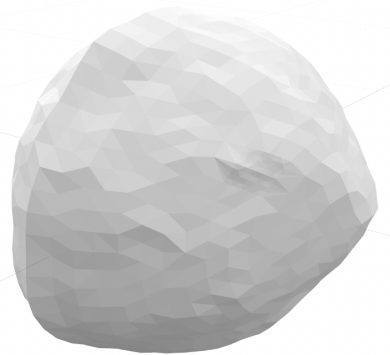


**Figure 15:** The shape model of the asteroid Bennu has been taken for simulations as there is no shape model yet for HO3 and both look alike. The asteroid HO3 as a mean radius of 20 meters, which makes it a very small asteroid.

The shape model of Bennu has been resized to fit the dimensions of HO3. To get a clearer grasp, it is interesting to compare two thermal maps with different revolution periods.

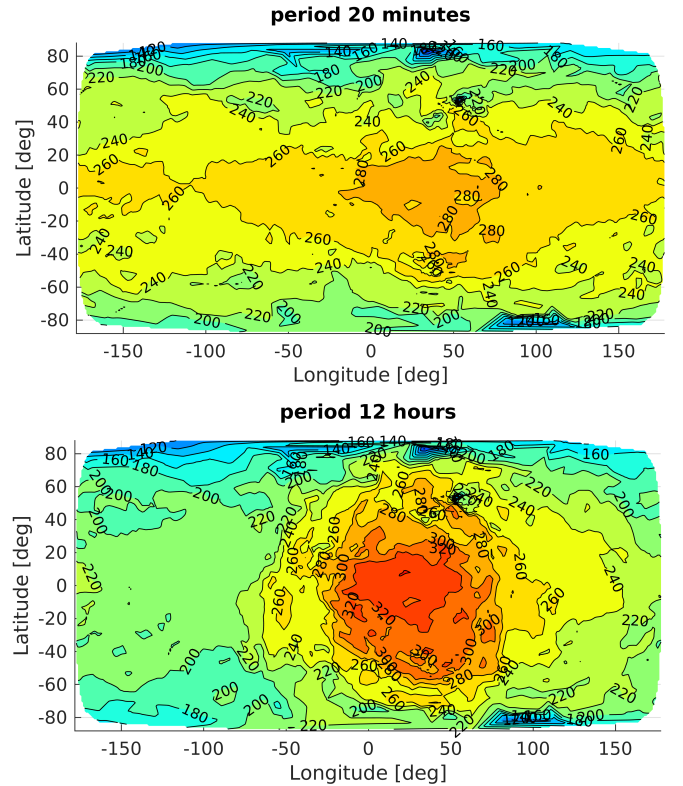


**Figure 16:** Impact of the revolution period of an asteroid on its temperature surface. Every other parameter has been set as in section 4. The model simply considers Eq. 1 without obliquity.

The difference between the two graphs is the extreme surface temperatures close to the equator. The faster the asteroid rotates, the less extreme the surface temperatures are at midday and midnight. The daily temperature at the equator varies within a range of 120 Kelvins with a revolution period of 12 hours, and only 20 Kelvins with a revolution period of 20 minutes. If the asteroid rotates slower, points on its surface stay longer in the day side and longer in the dark side. For

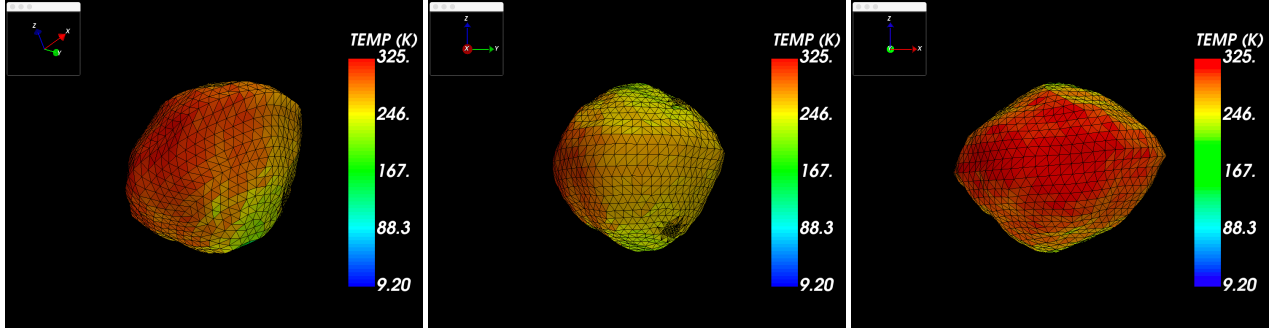


**Figure 17:** Thermal map of the surface temperatures applied on HO3 asteroid's shape model.

a fast rotating asteroid, the position on the asteroid matters less than for a slow rotating asteroid, as it get less influenced from the Sun orientation toward the position.

## 8. Influence of other parameters

For every simulation of this paper, orbital parameters and asteroid properties are referenced in subsection 4.3, except for comparison simulation in Fig. 14 with two different obliquities and in Fig. 16 with two different revolution periods. It might be essential to observe the change on the surface temperature when varying other parameters such as the thermal inertia and the heliocentric distance. The thermal camera needs and other tools on board rely on the changes in thermal inertia. Studying the evolution of the temperature with different heliocentric distances is important as the position of asteroids changes and especially Didymoon (from 1.1 AU to 1.9 AU). Juventas, a small satellite on board on the spacecraft Hera, and it has the mission to land on Didymoon to analyse the crater post impact formed by the DART mission. The range of landing is around 1.7 AU and 1.9 AU, and expected thermal inertia is in the range of 50—500 J K<sup>-1</sup> m<sup>-2</sup> s<sup>-1/2</sup>.

Results can be seen in Fig. 18. Variation of the thermal inertia impacts heat sensibility – pretty much as

variations of the revolution period seen in section 7. The higher the thermal inertia, the lesser the heat sensitivity and the lesser the temperature varies. The impact of the distance on temperature was predicted.

Further works in the study of the influence of the thermal inertia on the surface temperature lead to Fig. 19

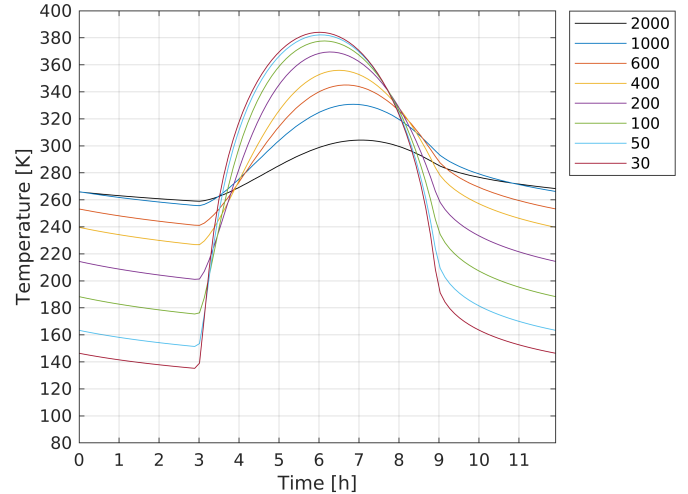


**Figure 19:** Influence of the thermal inertia on the daily surface temperatures. Simulation with an heliocentric distance of 1.0501 AU.

When the thermal inertia varies, the maximum and minimum surface temperature values change, as presented in Fig. 20.

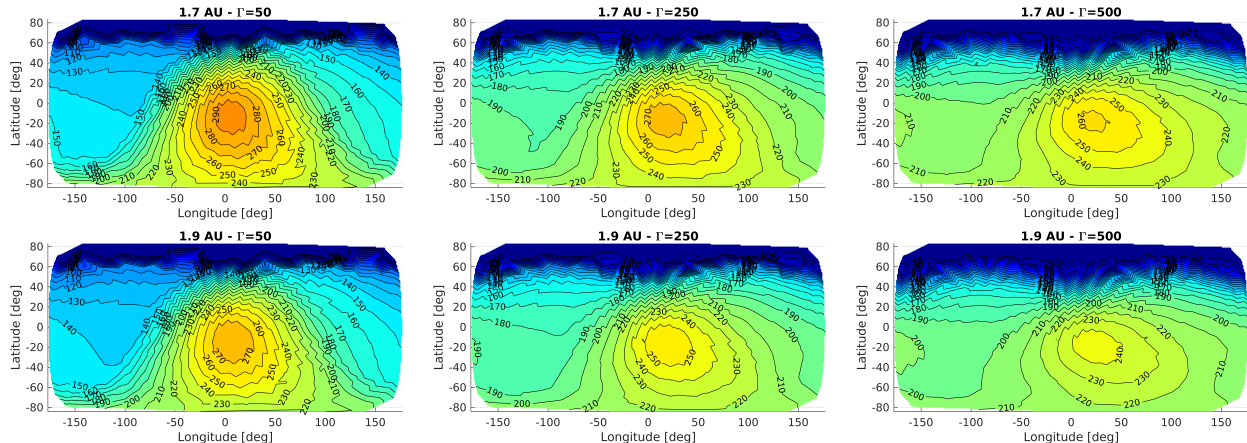


**Figure 18:** Thermal map of the surface temperature on Didymoon for different thermal inertia and heliocentric distance.

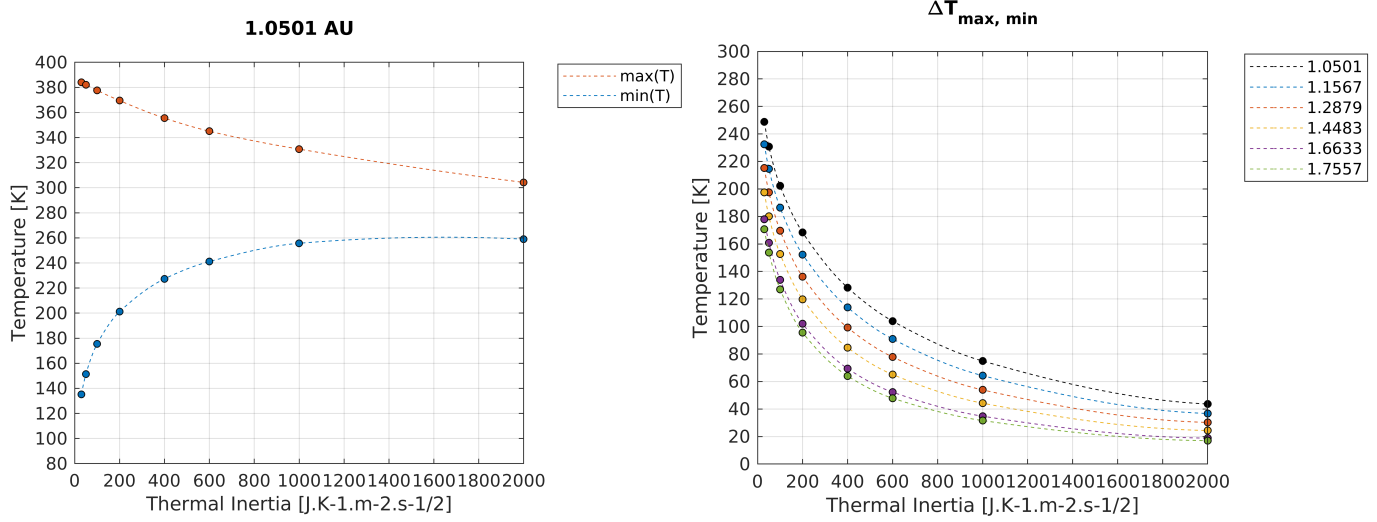


**Figure 20:** Influence of the thermal inertia on the maximum variations of the daily surface temperatures. Simulation in the first figure is for an heliocentric distance of 1.0501 AU. The second image shows the difference between the maximum and the minimum temperature for several distances.

## 9. Surface covering

In order to get a more visual grasp on HERA's vision on Didymoon, it is possible to make use of the NASA/NAIF Spice database, coupled with Cosmographia.

Spice is an observation geometry information system designed by NASA's Navigation and Ancillary Information Facility (NAIF) to assist scientists in planning and interpreting scientific observations from space-based instruments aboard planetary spacecraft.

Cosmographia is an interactive tool used to produce 3D visualizations of planet, spacecraft and other objects in the solar system, while taking into account trajectories positions and orientations.

By combining known positions of Didymoon, Didymain, expected positions of HERA and the characteristics of the on-board AFC – Asteroid Framing Camera, the objective is to recreate a visual representation of the visibility HERA will have on Didymoon during the various mission phases.

It relies on the FOV condition API set of functions – `cspice_fovray` – provided in the NAIF Spice toolkit which

verifies if a ray is within the boundaries of a specified instrument. By using this API, it is theoretically capable to determine which parts of Didymoon are visible at any moment in time.

A script has been written to reproduce the view of Fig. 21 in MATLAB for easier studies and it gives Fig. 22. The script detects whether Didymoon is outside the field of view of the framing camera as shown in Fig. 23.

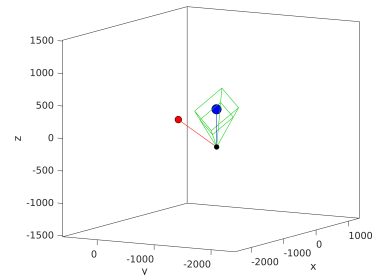


**Figure 23:** Example of the detection of the absence of Didymoon in the field of view of the framing camera. Didymoon appears in red as it is outside the field of view.

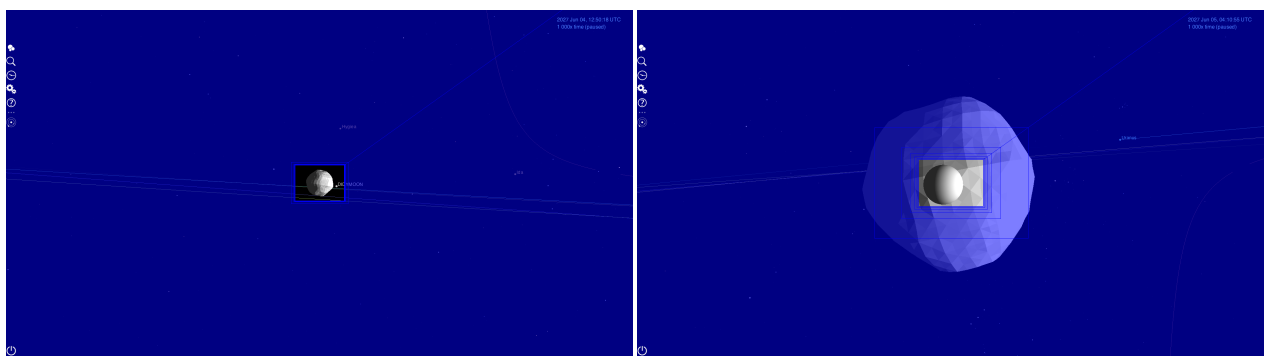


**Figure 21:** View from HERA on the binary system of asteroids Didymos from Cosmographia. The field of view of the camera imaging appears in blue. The first image is the previous rotation before the closest flyby on June 24, 2024, at 12:50, and the second image is during the closest flyby of 1 AU on June 25, 2024, at 4:00.

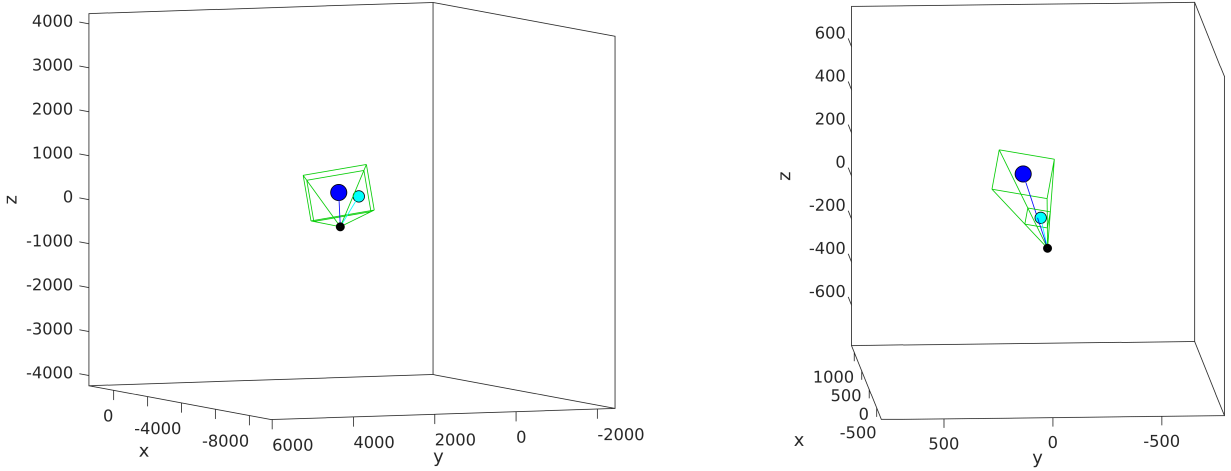


**Figure 22:** View from HERA on the binary system of asteroids Didymos reconstructed on MATLAB. The black dot is the spacecraft HERA, the cyan dot is Didymoon and the blue dot is Didymain. The two images are taken at the same time as in Fig. 21.

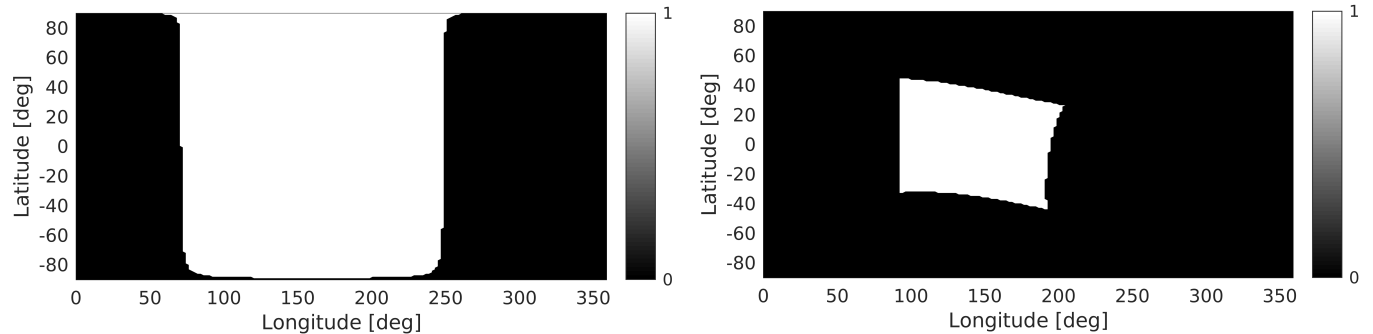


**Figure 24:** Percentage of visible surface of Didymoon. The two images are taken at the same time as in Fig. 21. The region in white represents the visible surface.

Fig. 22 and Fig. 23 show the results whether Didymoon is visible by the framing camera on board to HERA. Another aim of this document is to determine the percentage of visible surface. Fig. 24 shows the results.

There seems to be a small difference from the reality in the second image of Fig. 24. After studying the different possibilities to explain the cause, we have observed this weird-looking occurs only during the closest flyby of 1 AU. The visible surface is theoretically supposed to be the cross section of a sphere – this case actually happens when the observer is at infinite distance of the sphere. The visible surface tends to reach half of the sphere area. The closer the observer is to the object, the smaller the visible area must be. Further works will consist into studying this phenomenon.

## 10. Further works

A thermophysical model of the secondary in the Didymos system has been established. The case study performed covers the extreme thermal inertia range of  $50\text{--}2000 \text{ J K}^{-1} \text{ m}^{-2} \text{ s}^{-1/2}$  with heliocentric distances in the range of  $1\text{--}1.9 \text{ AU}$ , with and without obliquity. This

document also showed the impact of the revolution period on the surface temperatures. Calculations are based on shape models with triangular facets reduced to single points – medians of the facet – and their normals. After the previous study of Pelivan et al. (2017), we implemented the small neglected effects such as the mutual heating from the primary and the self heating. We observed the huge influence that the surface roughness plays on the temperature surfaces.

In addition to the HERA mission, we were asked to participate in the 2016 HO3 mission using our thermophysical model to understand what could be the temperatures to expect from a fast rotation small asteroid.

Ultimately, preliminary AFC viewing simulations have been carried out. An early estimation of the visible area on the secondary of the binary system of asteroids Didymos is now possible.

## Acknowledgements

We would like to express our sincerest appreciation to our supervisors at the Royal Observatory of Belgium,

Özgür Karatekin and Elodie Glosesener, as well as everyone who has been involved with us on our master thesis project since day one: Bart Van Hove and Zhu Ping from the Royal Observatory of Belgium, and Baptiste Rubino from IPSA. Thank you for accompanying us through this trip into the Solar System.

A huge thanks to everyone we met and with whom we discussed of the project. To our friends from the Observatory, Elisa Tasev, Amedeo Romagnolo, Alfonso Caldiero, Sébastien Le Maistre, Matthias Noeker.

To all admirable workers for ESA we had the chance to speak with, we think to Marc Costa Sitja, to Alessandro Zuccaro Marchi, to Ingeborg Joris.

## References

Clifford, S. M., and C. J. Bartels. The mars thermal model “Marstherm”, a fortran 77-finite differences program designed for general distribution. *Lunar Planet. Sci.*, XVII:142–143, 1986.

M. Delbo, M. Mueller, J. P. Emery, B. Rozitis, and M. T. Capria. Asteroid thermophysical modeling. *arXiv*, 2015.

Didymos reference model. Asteroid impact mission: Didymos reference model. reference document v3.1, ESA, 2015.

E. Glosesener. *Methane clathrate hydrate stability in the marsian subsurface and outgassing scenarios*. PhD thesis, UCLouvain, 2019.

H. Goldberg, C. Prioroc, and G.-R. G. team. Juventas mission analysis report (mar). Analysis report v1.0, GomSpace, 2019. JUV-GS-MAR-001.

P. Michel, A. Cheng, M. Küppers, P. Pravec, J. Blum, M. Delbo, S. Green, P. Rosenblatt, K. Tsiganis, J. Vincent, J. Biele, V. Ciarletti, A. Hérique, S. Ulamec, I. Carnelli, A. Galvez, L. Benner, S. Naidu, O. Barnouin, D. Richardson, A. Rivkin, P. Scheirich, N. Moskovitz, A. Thirouin, S. Schwartz, A. C. Bagatin, and Y. Yu. Science case for the asteroid impact mission (aim): A component of the asteroid impact & deflection assessment (aida) mission. *Advances in Space Research*, 2016.

I. Pelivan, L. Drube, E. Kührt, J. Helbert, J. Biele, M. Maibaum, B. Cozzoni, and V. Lommatsch. Thermophysical modeling of didymos’ moon for the asteroid impact mission. *Advances in Space Research*, 2017.

D. M. Williams and J. F. Kasting. Habitable planets with hight obliquities. *Icarus*, 1997.